The Astrophysical Journal, 866:125 (6pp), 2018 October 20 https://doi.org/10.3847/1538-4357/aadc67

The First Orbital Period of a Very Bright and Fast Nova in M31: M31N 2013-01b

Martino Marelli[1], Domitilla De Martino[2], Sandro Mereghetti[1], Andrea De Luca[1], Ruben Salvaterra[1], Lara Sidoli[1], Gianluca Israel[3], and Guillermo Rodriguez[3]
[1] INAF—Istituto di Astrofisica Spaziale e Fisica Cosmica Milano, via E. Bassini 15, I-20133 Milano, Italy; marelli@lambrate.inaf.it
[2] INAF—Osservatorio Astronomico di Capodimonte, Salita Moiariello 16, I-80131 Napoli, Italy
[3] INAF—Osservatorio Astronomico di Roma, Via Frascati 33, I-00040 Monteporzio Catone, Italy
Received 2018 August 4; revised 2018 August 14; accepted 2018 August 20; published 2018 October 19

Abstract

We present the first X-ray and UV/optical observations of a very bright and fast nova in the disk of M31, M31N 2013-01b. The nova reached a peak magnitude $R \sim 15$ mag and decayed by 2 mag in only 3 days, making it one of the brightest and fastest novae ever detected in Andromeda. From archival multiband data we have been able to trace its fast evolution down to $U > 21$ mag in less than two weeks and to uncover for the first time the super-soft X-ray phase, whose onset occurred 10–30 days from the optical maximum. The X-ray spectrum is consistent with a blackbody with a temperature of ∼50 eV and emitting radius of $\sim 4 \times 10^9$ cm, larger than a white dwarf (WD) radius, indicating an expanded region. Its peak X-ray luminosity, 3.5×10^{37} erg s^{-1}, places M31N 2013-01b among the most luminous novae in M31. We also unambiguously detect a short 1.28 ± 0.02 hr X-ray periodicity that we ascribe to the binary orbital period, possibly due to partial eclipses. This makes M31N 2013-01b the first nova in M31 with an orbital period determined. The short period also makes this nova one of the few known below the 2–3 hr orbital period gap. All of the observed characteristics strongly indicate that M31N 2013-01b harbors a massive WD and a very low mass companion, consistent with being a nova belonging to the disk population of the Andromeda galaxy.

Key words: galaxies: individual (M31) – novae, cataclysmic variables – stars: individual (M31N 2013-01b) – X-rays: binaries

1. Introduction

Classical novae (CNe) are close binary systems ($P_{\rm orb} \sim$ 1.5–10 hr) consisting of a late-type main sequence or red giant secondary and an accreting white dwarf (WD) primary that experience an outburst triggered by a thermonuclear runaway in the hydrogen-rich accreted material (Bode et al. 2008). CNe thus belong to the cataclysmic variable (CV) class. After a maximum brightening (up to 7–16 mag), the optical emission declines due to the receding photosphere at a rate that defines the nova speed class (Payne-Gaposchkin 1964). Part of the material is expelled at high velocities (Shore et al. 2011). The decline time, typically defined as the time needed to decline by 2 mag (t2), was found to be related to the peak maximum (Della Valle & Livio 1995) and to the expansion velocity of the ejected envelope (Della Valle et al. 2002; Schwarz et al. 2011; Shafter et al. 2011). Fast novae tend to be brighter and to display high expansion velocities.

After one to a few weeks, the receding atmosphere toward the hotter inner regions is such that the emission moves to X-rays, making the nova a super-soft X-ray source (SSS) with a temperature of the order of ∼20–80 eV and X-ray luminosities $>10^{36}$ erg s^{-1}. This phase is powered by stable hydrogen burning within the part of the accreted envelope and is observable when the ejected matter becomes optically thin to soft X-rays (Orio et al. 2001; Krautter 2002).

Few novae during the SSS phase were found to display short-period X-ray oscillations or quasi-oscillations on timescales of several tens of seconds with relatively short duty cycles (Beardmore et al. 2008; Ness et al. 2015), ascribed to *g-mode* pulsations of the burning envelope, which, if confirmed, have the potential to estimate the WD mass (see Ness et al. 2015; Wolf et al. 2018 and references within). Oscillations on timescales of thousands of seconds detected during the SSS phase have been interpreted as non-radial pulsations (Drake et al. 2003; Dobrotka & Ness 2010), while those found to be coherent signify the rotation period of a magnetic WD (Dobrotka & Ness 2010; Pietsch et al. 2011). On the other hand, periodic variations on longer (hour) timescales are compatible with the binary orbit, showing either eclipses (Sala et al. 2008) or X-ray modulations (Henze et al. 2010, 2014; Beardmore et al. 2012; Page et al. 2013).

Most Milky Way novae are found either in the Galactic bulge or lying in the Galactic plane, thus suffering from strong absorption. Novae in Local Group galaxies instead provide the best targets for studying outburst evolution and, in particular, the SSS phase. Because of its close distance (776 pc; Dalcanton et al. 2012; we will adopt this distance throughout this paper) and low Galactic extinction (Dalcanton et al. 2012) M31 is an ideal target for studying nova populations. Henze et al. (2010, 2014) published ∼25 novae (out of the ∼80 known) in M31 that show the SSS phase, covering the period until 2012. Only two of them, M31N 2006-04a and M31N 2011-11e, possess a candidate X-ray orbital period (1.6 h and 1.3 h, respectively), not confirmed due to the low statistics (Pietsch et al. 2011; Henze et al. 2014).

The Exploring the X-ray Transient and variable Sky (EXTraS) project (De Luca et al. 2016) developed new techniques and tools to extract and describe the timing behavior of archival X-ray sources detected by *XMM-Newton*/EPIC (Strüder et al. 2001; Turner et al. 2001). Because of the great improvement of EXTraS with respect to the 3XMM source catalog, we performed a systematic search for eclipsing and/or dipping sources in the *XMM-Newton* data set pointing to the M31 Galaxy, finding significant and periodic dips in the light

Table 1
Summary of the X-Ray and UV/Optical Simultaneous Observations of M31N2013

Instrument	OBS-ID	Optical/UV Band	Tstart	Exposure	L_{50}	Optical/UV Magnitude
…	…	…	Date(UTC)	(ks)	(10^{37} erg s^{-1})	(mag)
Swift	00032697001	U	2013 Feb 01 11:40:59	3.9	<3.6	18.84 ± 0.08
Swift	00032697002	U	2013 Feb-05 19:48:59	3.5	3.5 ± 1.3	19.85 ± 0.15
XMM-Newton	0701981201	UVW1	2013 Feb 08 21:55:52	24.0	3.3 ± 0.2	19.93 ± 0.38
Swift	00032697003	U	2013 Feb 09 13:42:58	3.9	1.8 ± 0.8	20.37 ± 0.18
Swift	00032697004	U	2013 Feb 13 07:39:59	3.8	<3.7	20.78 ± 0.35
Swift	00032697005	U	2013 Feb 17 04:27:59	4.0	<3.5	>21.9
Chandra/ACIS-I	14930	…	2013 Feb 18 08:02:31	3.9	<250	…
Swift	00032697006	UW1	2013 Feb 24 01:14:13	6.0	<2.6	>22.7
Chandra/HRC-I	14400	…	2013 Feb 24 10:38:42	5.1	<0.94	…
Swift	00032697007	UW2	2013 Feb 26 12:36:58	8.9	<1.9	>21.8
Swift	00032697008	UM2	2013 Mar 07 03:18:38	5.2	<3.3	>21.8
Chandra/HRC-I	15620	…	2013 Mar 11 23:03:17	5.1	<0.98	…
Chandra/ACIS-I	14931	…	2013 Mar 12 00:43:55	3.9	<250	…

Note. Here, we report for each observation the telescope, observation ID, the band in which optical/UV instrument was operating, the start time, and the exposure time. We also report the X-ray equivalent luminosity (see Section 3) and the average optical/UV magnitude for each observation. Errors are at 1σ; upper limits are at 3σ.

curve of 3XMM J004401.9 + 412544. The X-ray source is located at R.A. = $00^{h}\,44^{m}\,01\overset{s}{.}97$, decl.= $+41^{\circ}\,25'\,44\overset{''}{.}5$ (J2000)[4] (1σ statistical plus systematic error of $2''$), positionally consistent with the optical nova PNV J00440207 + 4125442 = M31N 2013-01b (henceforth M31N2013), located at R.A. = $00^{h}\,44^{m}\,02\overset{s}{.}09$, decl. = $+41^{\circ}25'\,44\overset{''}{.}4$ (J2000) ($5''$ statistical plus systematic error; Hornoch 2013). It was detected only once by *XMM-Newton* (out of 12 observations) on 2013 February 8, ∼14 days after the optical maximum reported by Hornoch (2013) and during a follow-up observation of the nova, thus confirming the association of the two sources.

M31N2013 was found as a bright optical transient (Hornoch 2013) on 2013 January 25.728 UT (this will be considered as T0 for the rest of the paper) with a peak R-band magnitude of 15.05(7). Follow-up observations[5] showed a rapid fading in a few days. M31N2013 was spectroscopically confirmed as a He/N or hybrid (Fe II b) nova by Shafter (2013), displaying broad (FWHM ∼ 5500 km s^{-1}) Balmer emission lines. The magnitude and X-ray luminosity (see Table 1) are consistent with a nova in M31, while excluding a foreground nova or a nova in our Galaxy (that would be much more or much less luminous than the other observed novae, respectively). It is located in the M31 disk (Hornoch 2013), further supporting the M31 membership.

During the optical decline, apart from *XMM-Newton*, M31N2013 was also observed with the *Neil Gehrels Swift* satellite (henceforth *Swift*) in the X-rays and UV and optical and the *Chandra* X-ray Observatory, using either HRC (Murray et al. 2000) or ACIS instruments (Nousek et al. 1998). Here, we present a complete analysis of the optical/UV and X-ray SSS phase of this nova, exploiting all of the available data. Section 2 describes the data reduction, Section 3 the analysis, and in Section 4 we discuss the results.

[4] 3XMM-DR8: http://xmmssc.irap.omp.eu/Catalogue/3XMM-DR8/3XMM_DR8.html.
[5] IAU CBAT: http://www.cbat.eps.harvard.edu/unconf/followups/J00440207+4125442.html.

2. Data Reduction

A 24 ks *XMM-Newton* ToO was dedicated to M31N2013 on 2013 February 8 (see Table 1). We made use of SAS v.15 to perform a standard data reduction from Observation Data Files, followed by a barycentrization to the solar system using the SAS tool `barycen`. For the timing analysis we only made the standard selection on pattern (0–4 for pn and 0–12 for MOSs), using the 0.2–1 keV energy band since the source is not detected above 1 keV. Pn and MOSs events were then added to perform the analysis. We then made use of the EXTraS tools and cuts[6] to study M31N2013 light curves in the 0.2–1 keV energy band. For the spectral analysis we used the entire EPIC data set, excluding high background periods (this reduced the exposure to ∼16 ks). The Optical Monitor (OM; Mason et al. 2001) data were reprocessed using the standard SAS tool `omichain`.[7] The transient was not detected by the Reflection Grating Spectrometers (RGS1,2; Den Herder et al. 2001).

The *Swift* XRT data of the eight observations (see Table 1) were processed with standard procedures using the Ftool (v.6.19) task `xrtpipeline`. We selected events with grades 0–12 and limited the analysis between 0.3 and 1.0 keV. The standard UVOT processing pipeline was used for the observations carried out with the UV filters, UW1, UW2, and UM2. We used the Heasoft tool `uvotmaghist` (taking into account the Small Scale Sensitivity check as recommended in the cookbook) to obtain a detection or an upper limit magnitude for each observation. The *Chandra* observations (see Table 1) were reprocessed using the *Chandra* Interactive Analysis of Observation (CIAO) software v4.5 with the `chandra_repro` task.

Table 1 reports the details of the X-ray and UV/optical simultaneous observations used in this paper.

3. Data Analysis

3.1. X-Ray Data

M31N2013 was selected among the 3XMM source list in M31 as one of the best eclipsing object candidates. We adopted

[6] http://www.extras-fp7.eu/index.php
[7] http://xmm-tools.cosmos.esa.int/external/sas/current/doc/

the spectral model used for the equivalent luminosity (see below) to convert EXTraS background-subtracted count rates into absorbed fluxes, then we made a weighted average of the flux light curve of each EPIC instrument to obtain a total flux light curve. We fitted a periodic eclipse model on the filtered 500 s flux light curve. Using an f-test, we found a significant improvement with respect to a constant model, with a chance probability of 3.4×10^{-6}. However, the model itself does not give a good representation of the light curve shape, giving null hypothesis probability (nhp) of 1.2×10^{-4}, indicating a more complex shape. We performed an independent search on pn plus MOSs events with a Rayleigh test on the *XMM-Newton* pn plus MOSs event list (Buccheri et al. 1983) over more than 9000 independent periods in the range 0.001–4.2 hr. This yielded a Z^2 value of 90 for $P = 1.29$ hr, which corresponds to a chance probability of 3×10^{-16} (taking into account the number of trials). We note that ∼75% of events come from pn. A similar analysis based on pn-only events still gives the periodicity at $>6\sigma$. To refine the period value we used a standard folding analysis based on the sum of pn and MOS counts into 10 phase bins. This resulted in a best period of $P = 1.28 \pm 0.02$ hr. All uncertainties are 1σ error as estimated following Leahy (1987).

We fitted the *XMM-Newton* spectra using an absorbed (abundances from Wilms et al. 2000) blackbody, obtaining a good fit (nhp = 0.16, d.o.f. = 37) with a column density $N_{\rm H} = (2.6 \pm 0.4) \times 10^{21}\,{\rm cm}^{-2}$ (in this paper, all o the uncertainties are at 1σ), a temperature $kT = (47 \pm 3)\,{\rm eV}$, an emission radius $R = 4.2^{+2.9}_{-1.6} \times 10^{9}\,{\rm cm}$, and an absorbed 0.2–10 keV flux of $(6.8 \pm 2.5) \times 10^{-14}\,{\rm erg\,cm^{-2}\,s^{-1}}$. For such a super-soft source, degeneration among parameters is expected and the flux cannot be de-absorbed correctly. In order to compare M31N2013 with the other novae from M31, we adopted the definition of "equivalent luminosity" L_{50} from Henze et al. (2014), obtained using a blackbody temperature $kT = 50\,{\rm eV}$ and the Galactic foreground absorption $N_{\rm H} = 6.7 \times 10^{20}\,{\rm cm}^{-2}$ (Henze et al. 2014). For M31N2013 we therefore obtain an unabsorbed flux of $(4.6 \pm 0.2) \times 10^{-13}\,{\rm erg\,cm^{-2}\,s^{-1}}$ that translates into $L_{50} = (3.3 \pm 0.2) \times 10^{37}\,{\rm erg\,s^{-1}}$. See also Figure 3.

The *XMM-Newton* light curve of M31N2013 has been folded using 20 bins (so that each bin has ∼50 counts; see Section 2) using the period obtained through the timing analysis (see Figure 1). The phased light curve shows a quasi-sinusoidal shape, even if the low significance of a constant plus sinusoidal model (nhp $= 4.2 \times 10^{-5}$, 17 d.o.f.) and of a simple eclipse model (nhp $= 4.6 \times 10^{-4}$, 16 d.o.f) points to a more complex behavior. Using a sinusoidal model, the pulsed fraction (defined as the normalization of the sinusoid over the constant) is $(40 \pm 5)\%$. The light curve also shows hints of a linear decrease with time (see Figure 2), but is not statistically significant (an f-test gives a chance probability for the improvement of 0.07).

In order to search for spectral variability, we extracted *XMM-Newton* spectra in two phase ranges, namely, 0.0–0.5 (off-pulse phase) and 0.5–1 (on-pulse phase). A spectral fit with all of the parameters tied except the normalization gives an acceptable fit, nhp = 0.98 d.o.f. = 30 ($R^{\rm off} = 3.1^{+1.5}_{-2.4} \times 10^{9}\,{\rm cm}$, $R^{\rm on} = 4.1^{+3.3}_{-1.8} \times 10^{9}\,{\rm cm}$). Similarly, leaving the column density free we obtain an acceptable fit, nhp = 0.96 d.o.f. = 30 ($N_{\rm H}^{\rm off} = (2.4 \pm 0.5) \times 10^{21}$, $N_{\rm H}^{\rm on} = (1.8 \pm 0.4) \times 10^{21}$). We also checked the spectra of the first and second half of the observation, obtaining again an acceptable fit. To further inspect possible spectral changes, we also produced hardness ratios (HRs) both phased (10 bins) and with time (one per orbital period) in the energy bands 0.2–0.4 keV and 0.4–0.7 keV. The HR distributions are consistent with a constant model. We therefore do not detect spectral variation with phase or time.

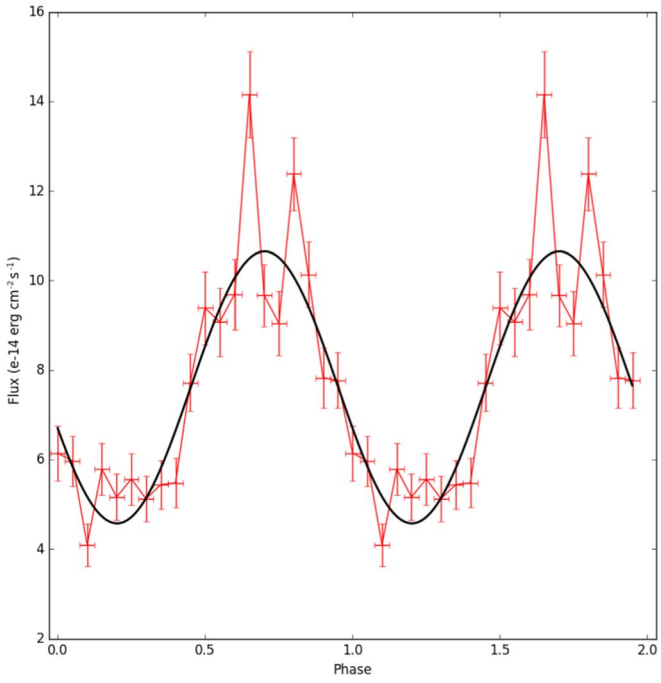

Figure 1. *XMM-Newton* phased light curve in the 0.2–1.0 keV range adopting the best-fit period of 4595 s. Count rates are converted to fluxes as detailed in Section 3. Here, we also report a sinusoidal fit (nhp $= 4.2 \times 10^{-5}$, 17 d.o.f.). Errors are at 1σ.

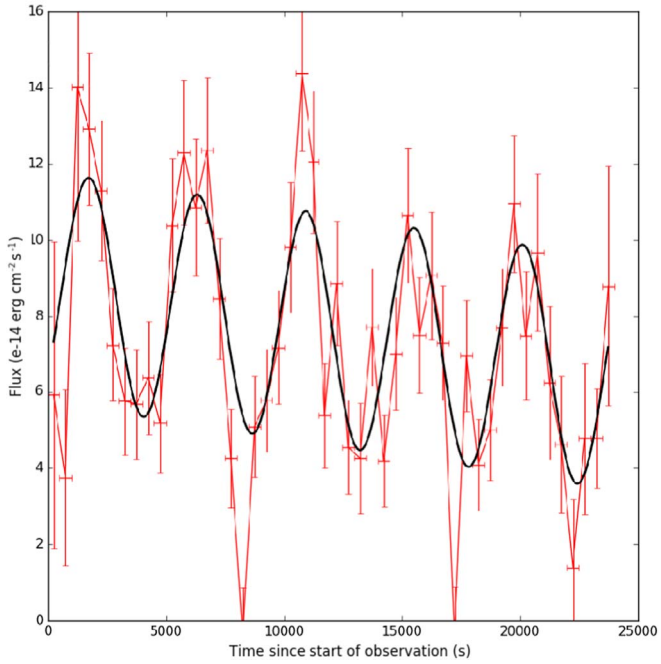

Figure 2. Time-resolved *XMM-Newton* light curve in the 0.2–1.0 keV range along with a sinusoidal plus linear fit (nhp $= 1.2 \times 10^{-4}$, 47 d.o.f.). Errors are at 1σ and bins are of 500 s. Fluxes are derived as described in Section 3. On the x-axis, we report time since 2013 February 8 UTC 21:55:52.

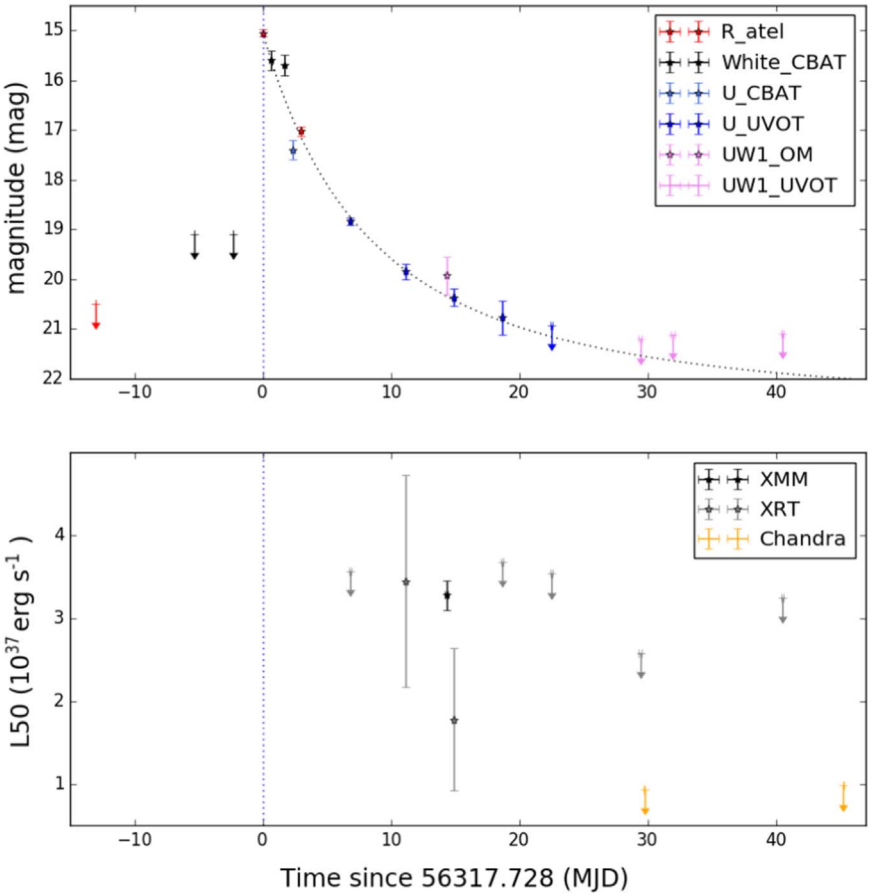

Figure 3. Long-term light curves of M31N2013. On the *x*-axis, we report time since the first detection of the nova. Upper panel: the UV/optical magnitudes clearly show an exponential decrease of the optical nova (dashed line) after the maximum (vertical dotted line). Lower panel: the equivalent X-ray luminosity L_{50}, as obtained from all X-ray instruments, instead shows a less clear decay of the X-ray source. Errors are at 1σ, and upper limits at 3σ.

Using the `ximage detect` Heasoft tool, we checked for source detection in all of the *Swift*/XRT observations. Obs.id. 00032697002 and 00032697003 revealed a source at the position of M31N2013 at 2.5σ. By adding the two images, we obtain a detection at 3.6σ. Although statistically poor, we consider these as detections due to the positional coincidence and the fact that the *XMM-Newton* detection is in between these two observations. The background-subtracted count rates were then converted into equivalent luminosities L_{50} of (3.5 ± 1.3) and (1.8 ± 0.8) $\times 10^{37}$ erg s^{-1}, respectively, taking into account the exposure map, effective area, and response matrix. For all of the other *Swift*/XRT observations we extracted a 3σ upper limit L_{50} using the definition of signal to noise. Similarly, we did not detect the X-ray counterpart in any of the *Chandra* data set, hence we derive 3σ upper limits to the L_{50} reported in Table 1 and Figure 3.

3.2. UV and Optical Data

A UV counterpart of M31N2013 is detected ($>3\sigma$) only during the first four *Swift*/UVOT observations and by the *XMM-Newton* OM (see Table 1), when the nova was brighter. There is a clear exponential decrease in the U band during the $\sim$12 days in which the source was detected. For the first three *Swift*/UVOT observations we also obtained the UVOT positions overlapping at 1σ and coincident with the optical position from Hornoch (2013) and Shafter (2013), (R.A., decl. J2000): $00^{h}44^{m}02\overset{s}{.}09$, $+41°25'44\overset{''}{.}29$ ($\pm 0\overset{''}{.}57$, systematic plus statistical error), $00^{h}44^{m}02\overset{s}{.}10$, $+41°25'\ 44\overset{''}{.}53$ ($\pm 0\overset{''}{.}57$), and $00^{h}44^{m}02\overset{s}{.}12$, $+41°25'\ 44\overset{''}{.}24$ ($\pm 0\overset{''}{.}62$).

To construct a long-term UV/optical light curve of M31N2013 we made use of the measurements reported in Table 2 and the *Swift*/UVOT and *XMM-Newton* OM data in Table 1. The long-term UV/optical light curve with all collected photometry is shown in the upper panel of Figure 3 along the X-ray equivalent luminosities L_{50} from *XMM-Newton*, *Swift*, and *Chandra*, reported in the lower panel. Bearing in mind that novae show different color decays and brightness at different wavelengths and we are using measurements from different filters, we estimate t_2 using a power-law fit to the composite long-term light curve. We derive $\alpha = 1.7$ and $t_2 = 2.8 \pm 0.2$ days, which is consistent with the simple difference between the two R-band measures (3.0 days).

4. Discussion

4.1. The X-Ray Periodicity

Our analysis of the *XMM-Newton* X-ray data resulted in a periodic modulation with a period of 1.28 ± 0.02 hr, obtained in an observation lasting about five cycles. The amplitude of this variability is large, $\sim$40%. The modulation appears to be also structured with hints of a double-peaked maximum and a flat minimum. The timescale and large amplitude of the modulation exclude that the SSS luminosity variation is due to pulsations (see Section 1). We ascribe the periodicity to the orbital period of the system. It is the first nova in M31 with an

Table 2
Summary of Optical Observations of M31N2013

Time UTC	Optical Band ...	Magnitude (mag)	References ...
2013 Jan 12 16:52:19.2	R	>20.5	(1)
2013 Jan 20 10:06:14.4	W	>19.1	(3)
2013 Jan 23 10:06:10.0	W	>19.1	(3)
2013 Jan 25 17:28:19.2	R	15.05 ± 0.07	(1)
2013 Jan 26 10:14:52.8	W	15.6 ± 0.2	(3)
2013 Jan 27 10:42:14.4	W	15.7 ± 0.2	(3)
2013 Jan 28 01:44:49.9	U	17.4 ± 0.2	(3)
2013 Jan 28 17:26:52.8	R	17.02 ± 0.09	(2)

Note. W refers to white (broadband) filter. CBAT data of January 27 do not report the error: we assumed the same error as the other measurement, so it should be taken with caution. References are: (1) Hornoch (2013); (2) Shafter (2013); (3) IAU CBAT[a].
[a] http://www.cbat.eps.harvard.edu/unconf/followups/J00440207+4125442.html.

orbital period unambiguously detected in the X-rays. Only candidate periods of two novae in M31 were found by Henze et al. (2010, 2014) during the SSS phase of M31N 2006-04a and M31N 2011-11e, 1.6 hr and 1.3 hr, respectively. The orbital period of CVs is an observational proxy of their evolutionary state, where the secular mass transfer rate decreases as the systems evolve toward short orbital periods (Howell et al. 2001; Barker & Kolb 2003). Hence, systems below the 2–3 hr orbital period gap (Warner 1995) are old systems and expected to accrete at a low rates $\lesssim 5 \times 10^{-11}\,M_{\odot}\,\mathrm{yr}^{-1}$ (Knigge et al. 2011). Assuming a 1.3 hr orbital period, the donor in M31N2013 is expected to be a very low mass ($M_2 \leqslant 0.1\,M_{\odot}$) star and of late M or even later spectral type (Knigge et al. 2011). Observed spectral types of CV donors at these short periods have been found to be late M dwarfs, M6–M9, as is the case for the short-period (1.4 hr) old novae CP Pup or GQ Mus (>M6; Szkody & Feinswog 1988). For L-type donors the systems could also be period bouncers and a few have been found so far with only one confirmed X-ray emitting magnetic system (Stelzer et al. 2017) accreting at very low rate ($\sim 10^{-14}\,M_{\odot}\,\mathrm{yr}^{-1}$). The very short 1.28 hr period locates M31N 2013-01b close to the expected theoretical orbital minimum of CVs (1.1 hr; Howell et al. 2001). Comparing the orbital period distribution of novae from Ritter & Kolb (2003) this nova is among the shortest orbital period systems and one of the few detected to display an orbital modulation in the SSS phase.

Orbital X-ray variability could be due to structures in the accretion disk, although absorption effects should be present. Additionally, a partial eclipse from fixed regions such as the disk-rim or by the donor star could be viable solutions. Similar partial eclipses were claimed for two Galactic novae, HV Cet (Beardmore et al. 2012) and V5116 Sgr (Sala et al. 2008). Both of the models require a high-inclination system ($i \gtrsim 60°$), Another possibility is that M31N2013 harbors a magnetic WD of the polar type (see Cropper 1990 for a review), where no disk is formed due to the high magnetic field of the WD primary ($B \geqslant 10$ MG) that locks its rotation at the orbital period. The polars show strong X-ray variations (up to 100%) due to localized accretion spots at the magnetic poles. However, the burning in the very early phases of a nova would rapidly reach a spherical symmetry, heating the whole WD surface (Casanova et al. 2010). The radius of the SSS emitting region is found to be in the range ~ 3–7×10^9 cm, which is indeed much larger than those of WDs, indicating an expanded emitting envelope. The lack of observed spectral variability along the phase may favor an eclipse, possibly partial, of the X-ray emitting region.

4.2. M31N 2013-Ib: A Very Fast Nova in M31

M31N2013 is a very fast nova, with a t_2 decay in the R band of ~3 days. The rate of decay is then $d\,m/d\,t \sim 0.7$ and is consistent with the universal law of Hachisu & Kato (2006) where the flux decays as $\mathrm{F} \propto \mathrm{t}^{-\alpha}$ with $\alpha = 1.7$–1.75. We find $\alpha = 1.7$. Lee et al. (2012) suggest that such very fast novae are more rarely encountered in M31 than in our Galaxy, even if selection effects should be taken into account. In particular, the online catalog of optical apparent novae in M31 by Pietsch & Haberl[8] reports a handful (11) of very fast novae with similar $t_2 \sim 2$–4 days. Fast novae are found to harbor massive WDs ($M_{\mathrm{WD}} \geqslant 1.2\,M_{\odot}$; Della Valle & Livio 1995; Della Valle et al. 2002) and the light curves are predicted to be almost independent of the chemical composition once iron content is fixed (Hachisu & Kato 2006).

The SSS X-ray turn-on and turn-off times cannot be fully constrained due to the lack of a deep monitoring shortly after the optical maximum. While the *Swift*/XRT upper limit on 2013 February 1 is too weak to constrain the turn-on time, the detections by *Swift*/XRT and *XMM-Newton* could hint to a fast turn-on $t_{\mathrm{on}} < 10$ days (taking into account the T0 reported in Section 1). The turn-off time could have occurred about one month after the optical maximum given the nondetection in the *Chandra* data, or before. Such short times are consistent with the correlation found between the turn-on and turn-off times found for M31 novae by Henze et al. (2014). The hot blackbody temperature as derived from the X-ray spectral fit is also in agreement with a short turn-off time on a similar timescale (see, e.g., Henze et al. 2014). Additionally, results from the M31N2013 data sets—including the short t2, the extremely high expansion velocity detected in the optical spectrum of the early phases of the outburst (Shafter 2013), turn-on and turn-off times—appear to be consistent with the relations found for the M31 novae (Henze et al. 2014). Although consistent, in all of these graphs M31N2013 is always at the edge of the relationships, owing to its short t2, turn-on time, and turn-off time, thus allowing for a better constraint of the link among these quantities. The X-ray luminosity of the SSS of M31N2013 is consistent with the other M31 novae found so far ($L_{50} < 8.7 \times 10^{37}$ erg s^{-1}; Henze et al. 2014), although it is in the bulk of the most luminous ones (only 4 out of the 24 M31 novae reported in Henze et al. 2014 show a higher L_{50}).

Using the dust maps by Montalto et al. (2009) that include the contribution of the Galactic foreground extinction ($E_{\mathrm{gal}}(B-V) = 0.10$), we derive a total extinction $0.10 \lesssim E(B-V) \lesssim 0.21$, since the location of M31N2013 within M31 is not known. This translates into a range of extinction in the R band of $0.26 \leqslant A_R \leqslant 0.55$. Assuming a distance of 776 ± 18 kpc and this range of extinction, we estimate an absolute magnitude at the peak of the optical light curve in the range $-9.60 \leqslant M_R \leqslant -10.0$. This range is fully consistent with the absolute peak magnitude observed in fast novae with similar t_2 and in particular with the super-bright Galactic nova

[8] http://www.mpe.mpg.de/~m31novae/opt/m31/index.php

V1500 Cyg (Kato et al. 2013). Unfortunately, due to the loosely constrained optical and X-ray positions, search results for the nova progenitor were inconclusive.

Although not studied until now, M31N2013 is one of the brightest and fastest nova ever detected in M31, belonging to the disk population and likely harboring a massive WD, one of the few known at very short orbital periods.

The authors acknowledge financial support from ASI under ASI/INAF agreement No. 2017-14.H.0. This work was supported by the Fermi contract ASI-INAF I-005-12-0. We acknowledge financial support from the Italian Space Agency (ASI) through the ASI-INAF agreement 2017-14-H.0.

Facilities: XMM, *CXO*, *Swift*.

ORCID iDs

Martino Marelli https://orcid.org/0000-0002-8017-0338
Domitilla De Martino https://orcid.org/0000-0002-5069-4202
Sandro Mereghetti https://orcid.org/0000-0003-3259-7801
Ruben Salvaterra https://orcid.org/0000-0002-9393-8078
Lara Sidoli https://orcid.org/0000-0001-9705-2883
Gianluca Israel https://orcid.org/0000-0001-5480-6438

References

Barker, J., & Kolb, U. 2003, MNRAS, 340, 623
Beardmore, A. P., Osborne, J. P., Page, K. L., et al. 2008, in ASP Conf. Ser. 401, RS Ophiuchi (2006) and the Recurrent Nova Phenomenon, ed. A. Evans et al. (San Francisco, CA: ASP), 296
Beardmore, A. P., Osborne, J. P., Page, K. L., et al. 2012, A&A, 545, 116
Bode, M. F., & Evans, A. 2008, Classical Novae (Cambridge: Cambridge Univ. Press)
Buccheri, R., Bennett, K., Bignami, G. F., et al. 1983, A&A, 128, 245
Casanova, J., José, J., García-Berro, E., Calder, A., & Shore, S. N. 2010, A&A, 513, L5
Cropper, M. 1990, SSRv, 54, 195
Dalcanton, J. J., Williams, B., F., Lang, D., et al. 2012, ApJS, 200, 18
De Luca, A., Salvaterra, R., Tiengo, A., et al. 2016, in The Universe of Digital Sky Surveys, ed. N. R. Napolitano et al. (Cham: Springer International), 291
Della Valle, M., & Livio, M. 1995, ApJ, 452, 704
Della Valle, M., Pasquini, L., Daou, D., & Williams, R. E. 2002, A&A, 390, 155
Den Herder, J. W., Brinkman, A. C., Kahn, S. M., et al. 2001, A&A, 365, L7
Dobrotka, A., & Ness, J.-U. 2010, MNRAS, 405, 2668
Drake, J. J., Wagner, R. M., Starrfield, S., et al. 2003, ApJ, 584, 448
Hachisu, I., & Kato, M. 2006, ApJS, 167, 59
Henze, M., Ness, J.-U., Darnley, M. J., et al. 2014, A&A, 563, A2
Henze, M., Pietsch, W., Haberl, F., et al. 2010, A&A, 523, 89
Hornoch, K. 2013, ATel, 4765
Howell, S. B., Nelson, L. A., & Rappaport, S. 2001, ApJ, 550, 897
Kato, M., Hachisu, I., & Henze, M. 2013, ApJ, 779, 19
Knigge, C., Baraffe, I., & Patterson, J. 2011, ApJS, 194, 28
Krautter, J. 2002, in AIP Conf. Proc. 637, Classical Nova Explosions, ed. M. Hernanz & J. Jose (Melville, NY: AIP), 345
Leahy, D. A. 1987, A&A, 180, 275
Lee, C.-H., Riffeser, A., Seitz, S., et al. 2012, A&A, 537, A43
Mason, K. O., Breeveld, A., Much, R., et al. 2001, A&A, 365, L36
Montalto, M., Seitz, S., Riffeser, A., et al. 2009, A&A, 507, 283
Murray, S. S., Austin, G. K., Chappell, J. H., et al. 2000, Proc. SPIE, 4012, 68
Ness, J.-U., Beardmore, A. P., Osborne, J. P., et al. 2015, A&A, 578, 39
Nousek, J. A., Townsley, L. K., Chartas, G., et al. 1998, Proc. SPIE, 3444, 225
Orio, M., Covington, J., & Ögelman, H. 2001, A&A, 373, 542
Page, K. L., Osborne, J. P., Wagner, R. M., et al. 2013, ApJ, 768, L26
Payne-Gaposchkin, C. 1964, The Galactic Novae (New York: Dover Publication)
Pietsch, W., Henze, M., Haberl, F., et al. 2011, A&A, 531, A22
Ritter, H., & Kolb, U. 2003, A&A, 404, 301
Sala, G., Hernanz, M., Ferri, C., & Greiner, J. 2008, ApJL, 675, L93
Schwarz, G. J., Ness, J.-U., Osborne, J. P., et al. 2011, ApJS, 197, 31
Shafter, A. W. 2013, ATel, 4768
Shafter, A. W., Darnley, M. J., Hornoch, K., et al. 2011, ApJ, 734, 12
Shore, S. N., Augusteijn, T., Ederoclite, A., & Uthas, H. 2011, A&A, 533, 8
Stelzer, B., de Martino, D., Casewell, S. L., Wynn, G. A., & Roy, M. 2017, A&A, 598, L6
Strope, R. J., Schaefer, B. E., & Henden, A. A. 2010, AJ, 140, 34
Strüder, L., Briel, U., Dennerl, K., et al. 2001, A&A, 365, L18
Szkody, P., & Feinswog, L. 1988, ApJ, 334, 422
Turner, M. J. L., Abbey, A., Arnaud, M., et al. 2001, A&A, 365, L27
Warner, B. 1995, Cataclysmic Variable Stars, Cambridge Astrophysics Series, Vol. 28 (Cambridge: Cambridge Univ. Press)
Wilms, J., Allen, A., & McCray, R. 2000, ApJ, 542, 914
Wolf, W. M., Townsend, R. H. D., & Bildsten, L. 2018, ApJ, 855, 127